Acceleration Waves in Cylindrical Shrinking Gas Bubbles

Acceleration waves in cylindrical shrinking gas bubbles

Francesca Brini,[*,a] and Leonardo Seccia[a]

[a] *University of Bologna, Department of Mathematics and AM², via Saragozza, 8 - Bologna - Italy*

[*]Email: francesca.brini@unibo.it

Number of pages:	29
Number of tables:	0
Number of figures:	5

Abstract

The paper studies the case of shrinking cylindrical gas bubbles, acting as a radial piston and generating acceleration waves. The behaviour of such waves and their improbable transformation into shocks are illustrated theoretically, as well as through some examples inspired by experimental data. The use of rational extended thermodynamics enables us to highlight the relevance of the dissipation and the possible role played by dynamic pressure and stress tensor in bubble evolution or shock formation. These results constitute an extension and a completion of a previous work dedicated to the analysis of acceleration waves generated in oscillating spherical bubbles.

Keywords — Acceleration waves, cylindrical oscillating gas bubbles, polyatomic gases, dynamic pressure, rational extended thermodynamics

I. INTRODUCTION

Since the beginning of last century, gas bubbles generated in a liquid and oscillating in a non-linear way, for example in response to an acoustic signal or to a pressure impulse, have been the topic of many researches, both theoretical and experimental. As a matter of fact, they undoubtedly represent an amazing subject due to the surprising effects associated with their dynamics and to the multitude of applications in the most varied fields of science and technology, covering a large range of length scales [1].

After the pioneering studies by Lord Rayleigh [2] in 1917, the literature about bubbles has been increasing exponentially and it is not possible to recall all the papers and books devoted to this subject. We only mention some general reviews [1, 3–8], underling that this is not a complete reference list. Cavitation frequently involves the formation of a multi-bubble structure. Yet, in many experimental configurations a clearer understanding of the countless bubble phenomena is favoured by analysing a single one, generated in a liquid through different techniques (like the irradiation with standing acoustic wave or a focused laser pulse). In many cases it is assumed that bubbles present a perfect spherical shape, but it is well known that non-spherical bubble walls can develop during the phases of growth and collapse [1, 5, 9]. Among the possible shapes, there are many recent papers describing the dynamics of cylindrical bubbles [10, 11], that are modelled by an extension of the Rayleigh-Plesset equation in the limit of two space dimensions [9]. Specifically, cylindrical bubbles were observed in confined geometries, such as parallel flat plates [12, 13], subtle organic structures like capillaries [14, 15], or microfluidic systems (the so-called lab-on-a-chip devices) [16–20]. In this last case, very important for several applications to microfluidic devices, a laser-induced cavitation bubble is created inside microscopic narrow gaps. Initially its form may be considered approximately spherical, if the bubble is at the gap centre, far from boundaries, and if the parameters of the system are carefully controlled [20]. Then, the bubble grows to become cylindrical at its maximum volume. This happens if its diameter overcomes the height of the channel, but remains lower of its width. Finally, the bubble collapses conserving its cylindrical symmetry.

The bubble oscillation can act as a radial piston on the gas, causing the formation of an acceleration wave (AW, also called weak discontinuity); in other words a propagating surface across which all the field variables are continuous, but not their first derivatives [21–23]. AWs are

observed in different physical frameworks and in several materials, however in the present work we concentrate on polyatomic gases. In gases AWs are generated by a suitable perturbation, such as that of a piston during its accelerated motion [24–31]. An interesting question associated with this topic is the potential AW degeneracy into shock waves. One speaks of stability or lack of stability of the physical system if the AWs do not or do transform into a discontinuity wave [27]. In particular, it was proved that the PDEs describing the gas dynamics should exhibit both hyperbolicity and dissipation property, in order to make the transformation into a shock not only possible, but also compatible with experimental observations [32]. A model of hyperbolic balance laws with dissipative terms usually predicts the existence of a critical value of the initial AW amplitude, below which no shock formation is possible [22, 23, 26–29, 33].

To study AW evolution in cylindrical gas bubbles we refer to Rational Extended Thermodynamics (from now on RET). This recent theory was developed firstly for rarefied monatomic gases [34] and then expanded to polyatomic gases by Ruggeri, Sugiyama, Arima and Taniguchi [33, 35]. Its novelty with respect to other theories must be sought in the independent field variables taken into consideration. As a matter of fact, non-equilibrium variables (for instance stress tensor, dynamic pressure and heat flux) are seen as independent fields in the same way as the usual mass density, momentum and energy. Moreover, the field equation system is composed by hyperbolic balance laws and satisfies universal physical principles like relativity and entropy principles. The well-known Grad 13-moment model is a particular RET example valid for monatomic rarefied gases. In many cases, RET has predicted phenomena in accordance with experiments, in particular when the effects take place under non-equilibrium conditions [33, 34]. In [36] we applied RET to the bubble framework for the first time, and the present work represents an extension of the previous analysis to the case of cylindrical bubbles.

The paper is organized as following. In Section II we summarize the main ideas about oscillating gas bubbles with particular attention to the cylindrical case. The AW theory is illustrated in Section III, while Section IV is devoted to the RET theory. The AW evolution inside the bubble is investigated in Section V, while some physical examples are presented in Section VI. The conclusions are summarized in the last section.

II. DYNAMICS OF AN OSCILLATING GAS BUBBLE IN A MICROCHANNEL

In the last decades many papers and books presented theoretical and experimental studies about gas bubbles oscillating within a liquid in the presence of an external acoustic field. If the bubble is away from the container walls, it is commonly supposed to keep a perfect spherical shape and the dynamic of the bubble radius $R = R(t)$ (if t is the time variable) is described by a non-linear ordinary differential equation. If the liquid around the bubble can be seen as incompressible, one usually refers to the Rayleigh-Plesset equation or to one of its variants [5, 8]:

$$R\ddot{R} + \frac{3}{2}\dot{R}^2 = \frac{1}{\rho_L}\Big(P_i - P_e\Big) = \frac{1}{\rho_L}\Big(P_g(R) - P_\infty + P_a(t) - \frac{4\eta\dot{R}}{R} - \frac{2\varsigma}{R}\Big) + \frac{R}{\rho_L c_L}\frac{d}{dt}(P_g(R) + P_a(t)), \tag{1}$$

where $\dot{R} = dR/dt$, $\ddot{R} = d^2R/dt^2$, P_e and P_i indicate the external pressure in the liquid and the internal pressure in the gas respectively, ρ_L is the mass density of the liquid, c_L is the sound velocity in the liquid around the bubble. The shear viscosity and the surface tension of the liquid are denoted by η and ς. Moreover, the gas pressure in the bubble is P_g, the external acoustic field is denoted by P_a, while P_∞ is the constant undisturbed liquid pressure far from the bubble (in spherical geometry an infinite distance is taken into account), which coincides with ambient atmospheric pressure. Although relation (1) is determined imposing that the bubble radius varies slower than the sound speed (both in the liquid, c_L and in the gas, c_g), it was verified that it could be employed also in a supersonic case when $\dot{R} \gg c_g$ and/or $\dot{R} \gg c_L$ [4, 5, 37]. To derive (1) it is also implicitly assumed that the gas pressure is spatially uniform within the bubble (the so called "homobaric" hypothesis). Actually, a non-vanishing acceleration of the bubble radius is not compatible with a perfectly homogenous pressure, but it is was proved that the spatial dependence of P_g can be physically neglected in many cases, and it is coherent with (1) [6, 38–40].

Equation (1) can be closed and numerically solved, imposing that the gas pressure is a known function of the bubble radius, compatible with an isothermal or an adiabatic regime [6]. Alternatively, one can integrate the Rayleigh-Plesset equation coupled with the PDE system that models the gas behaviour inside the bubble. This second approach is obviously more accurate, but also much more computationally heavy [39–42]. If a periodic acoustic field like $P_a = P'_a \cos(\omega_a t + \phi)$ is imposed to the system, the behaviour of the radius of a spherical bubble can be qualitatively

illustrated in Figure 1(a): the initial value of $R(t=0) = R_E$ corresponds to the equilibrium radius, i.e. the bubble radius in the absence of the external sound. Switching on P_a, different phases can be observed: an initial expansion of the bubble that reaches its maximum radius R_M and a consecutive shrinkage up to the minimum radius $R_m < R_E$. The last part of the contraction turns out to be very rapid and sometimes very violent, reaching values of R_m comparable with the van der Waals hard core radius [1, 5–8]. The phenomenon comes always with bouncing damped oscillations.

During the first phase of the contraction, when $R_M > R > R_E$, (1) is usually simplified, neglecting the gas pressure P_g, the acoustic pressure P_a and their variations, the viscous term and the surface tension, so that it is assumed [4, 5, 37]

$$\frac{1}{2}R^3\dot{R}^2 = \frac{P_\infty(R_M^3 - R^3)}{3\rho_f}. \tag{2}$$

In many experiments it was analysed the case of an initially spherical (or semi-spherical) bubble generated in a narrow channel, in the presence of an external sound field. It was observed that the close proximity to a wall influences the bubble's evolution. In particular, if the bubble expands to a size greater than the distance between the walls, it transforms into a cylindrical shape and the subsequent contraction should be modelled by an ODE derived similarly as the Rayleigh-Plesset one, but capable of describing bidimensional radial phenomena [9]:

$$(R\ddot{R} + \dot{R}^2)\log(R/R_\infty) + \frac{1}{2}\dot{R}^2\left(1 - \frac{R^2}{R_\infty^2}\right) = \frac{P_\infty - p_B}{\rho_L}. \tag{3}$$

We stress that (3) was introduced to model the effect of a radial symmetric shell of incompressible fluid, whose radius goes from $R(t)$ (the time-dependent cylindrical bubble radius) to $R_\infty > R(t)$ (at which the velocity of the fluid is zero). Moreover, in (3) P_∞ denotes the unperturbed liquid pressure at R_∞ (here R_∞ cannot tend to infinity) and p_B represents the pressure in the bubble. If one neglects the thermodynamics inside the bubble, the possible acoustic signal, the viscosity terms and the contribute due to the surface tension, (3) can be simplied as [9, 16]

$$(R\ddot{R} + \dot{R}^2)\log\left(\frac{R}{R_\infty}\right) + \frac{1}{2}\dot{R}^2 = \frac{P_\infty}{\rho_L}. \tag{4}$$

(a) **(b)**

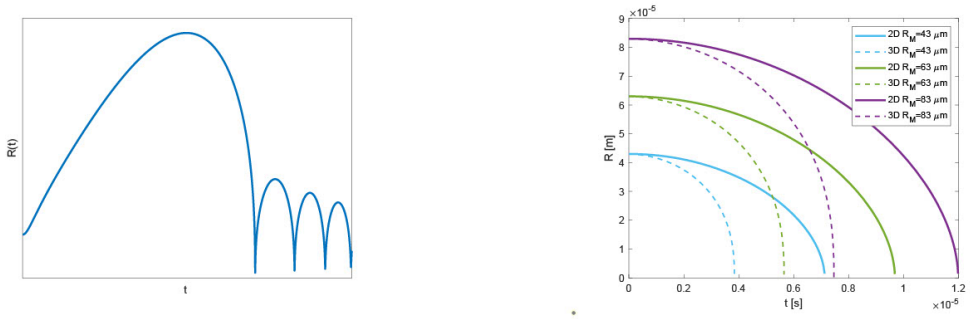

Fig. 1. In (a) the behaviour of the radius in a spherical bubble, described by Rayleigh-Plesset equation. In (b) a comparison between spherical (3D) and cylindrical (2D) gas bubbles for different maximum radii.

Comparisons with experimental data show a good agreement between (4) and the detected bubble radius evolution [16–18] if the maximum radius, R_M, is not too large. No bouncing oscillations were observed. Figure 1(b) shows a qualitative comparison between the radius contraction in spherical and cylindrical bubbles described by (2) and (4). In agreement with the experimental results, the shrinkage of cylindrical bubbles turns out to be much slower than that in a spherical domain, never reaching a supersonic regime. The comparison is proposed for the same values of R_M: in continuous line the radius of the cylindrical bubble, in dashed line that of the spherical bubble.

As already remarked in the literature (see for instance [43]) and studied in [36], a contracting bubble could act on the gas as a radial piston, giving rise to a radial acceleration wave under particular circumstances.

III. ACCELERATION WAVES

One faces an acceleration wave (AW) when dealing with a propagating surface Γ across which all the field variables are continuous, but at least one of them exhibits a jump in its derivative.

Hence, if $\mathbf{u}$ represents the field vector, $\varphi(\mathbf{z},t)=0$ is the equation of Γ and $[\![\cdot]\!]=(.)_{\varphi=0^-}-(.)_{\varphi=0^+}$ denotes a jump across such a wave front, for an AW it must hold $[\![\mathbf{u}]\!]=\mathbf{0}$, while $[\![\frac{\partial \mathbf{u}}{\partial \varphi}]\!]=\boldsymbol{\mathcal{A}}\neq\mathbf{0}$ [21]. Referring to a one-dimensional wave and a one-dimensional hyperbolic set of field equations of the form

$$\partial_t\mathbf{u}+\mathbf{B}(\mathbf{u},z,t)\partial_z\mathbf{u}=\mathbf{T}(\mathbf{u},z,t), \tag{5}$$

it was proved that [21–23]

- The velocity normal to the wave front $V=-\varphi_t/|\nabla\varphi|$ coincides with a characteristic speed λ of system (5) evaluated in the unperturbed field: $V=\lambda(\mathbf{u}_u)$.
- The jump vector $\boldsymbol{\mathcal{A}}$ is proportional to the right eigenvector $\mathbf{r}$ (of matrix $\mathbf{B}$) corresponding to λ, evaluated in $\mathbf{u}_u$, so that $\boldsymbol{\mathcal{A}}=\mathcal{A}\mathbf{r}(\mathbf{u}_u)$.
- The scalar amplitude $\mathcal{A}$ satisfies the Bernoulli equation: $\frac{d\mathcal{A}}{dt}+a(t)\mathcal{A}^2+b(t)\mathcal{A}=0$, where d/dt denotes the time derivative along the characteristic line ($dx/dx=\lambda(\mathbf{u_u})$) and coefficients $a(t)$ and $b(t)$ depend on time.

  The expression of the scalar amplitude as a function of t turns ot to be

$$\mathcal{A}(t)=\frac{\mathcal{A}(0)g_1(t)}{1+\mathcal{A}(0)g_2(t)},\quad \text{with } g_1(t)=\exp\left(-\int_0^t b(s)ds\right)\quad \text{and}\quad g_2(t)=\int_0^t a(s)g_1(s)ds, \tag{6}$$

where $\mathcal{A}(0)$ is the initial values of $\mathcal{A}$ when $t=0$.

The Bernoulli's coefficients a and b, for one-dimensional waves and for a set of PDEs written as (5), read [21–23]

$$\begin{aligned} a(t)&=\varphi_z(t)(\nabla_{\mathbf{u}}\lambda\cdot\mathbf{r})\Big|_u,\\ b(t)&=\left\{\mathbf{r}((\nabla_{\mathbf{u}}\mathbf{l})^T-\nabla_{\mathbf{u}}\mathbf{l})\cdot\frac{d\mathbf{u}}{dt}+(\nabla_{\mathbf{u}}\lambda\cdot\mathbf{r})(\mathbf{l}\cdot\mathbf{u}_z)-\nabla_{\mathbf{u}}(\mathbf{l}\cdot\mathbf{T})\cdot\mathbf{r}+\mathbf{l}\cdot\frac{\tilde{d}\mathbf{r}}{dt}\right\}\Big|_u, \end{aligned} \tag{7}$$

where $w_z=\partial w/\partial z$ for any w and $\nabla_{\mathbf{u}}\cdot=\partial\cdot/\partial\mathbf{u}$. In addition, $\mathbf{l}(\mathbf{u},z,t)$ and $\mathbf{r}(\mathbf{u},z,t)$ indicate the left and right eigenvector of $\mathbf{B}$ associated with the eigenvalue λ. For any function w of the field variables we refer to the notation: $w|_u=w(\mathbf{u}_u)$, while $\frac{d\cdot}{dt}=\partial_t\cdot+\lambda_u\partial_z\cdot$ and $\frac{\tilde{d}\cdot}{dt}=(\frac{d\cdot}{dt})|_{\mathbf{u}=const}$.

In the models that we are going to employ in the next Sections, the second component of $\mathbf{u}$

corresponds always to the gas velocity v along the z-direction. Moreover, we will focus on the AW propagating with a non-vanishing velocity. Therefore, we determine the left and right eigenvectors, $\mathbf{l}$ and $\mathbf{r}$ in such a way that $\mathbf{l}\cdot\mathbf{r} = 1$ (this requirement is necessary to make valid the previous points), and $r_2(\mathbf{u}_u) = -\frac{1}{\lambda_u}$, so that the scalar amplitude $\mathcal{A}$ always satisfies the Hadamard condition [31,36].

Hyperbolic sets of PDEs present often different non-zero characteristic speeds and different propagating AWs could be observed simultaneously. Usually the focus is restricted to the fastest one, since it is the only wave travelling into the unperturbed solution $\mathbf{u} = \mathbf{u}_u$.

Concerning the behaviour of $\mathcal{A}$, it is well-known [21–23] that for an AW that satisfies the condition $\frac{\partial\lambda}{\partial\mathbf{u}}\cdot\mathbf{r} \neq 0$ and for any suitable initial values $|\mathcal{A}(0)| > |\mathcal{A}_{cr}|$, there exists a critical time t_{cr} such that the AW degenerates into a shock wave and the field variables present jumps across Γ. Moreover, it is possible to prove that $\mathcal{A}_{cr} = -\lim_{t\to\infty} 1/g_2(t)$. The present work focuses on incoming cylindrical waves travelling towards the axis. In this context, we define the time t_* such that $x(t_*) = 0$ and necessarily the critical scalar amplitude becomes $\mathcal{A}_{cr} = -\lim_{t\to t_*} 1/g_2(t)$. For the sake of simplicity, we neglect in the following analysis the possible interaction between the AW and the bubble boundaries.

IV. RATIONAL EXTENDED THERMODYNAMICS MODELS

For a rarefied polyatomic gas it is possible to refer to kinetic theory [44] and introduce a generalized Boltzmann equation [45], requiring that the distribution function depends not only on time (t), space ($\mathbf{z} = (z_1, z_2, z_3)$) and microscopic velocity ($\mathbf{c} = (c_1, c_2, c_3)$), but also on the continuous variable I ($I \in [0, \infty)$) that accounts for the internal modes of the molecules. Such a function ($f = f(t, \mathbf{z}, \mathbf{c}, I)$) satisfies a Boltzmann equation with the same structure as in a monatomic case [45]:

$$\partial_t f + \sum_{j=1}^{3} c_j \partial_j f = Q, \tag{8}$$

where Q denotes the collision term, and $\partial_t \cdot = \partial\cdot/\partial t$, $\partial_j \cdot = \partial\cdot/\partial z_j$.

RET theories for rarefied polyatomic gases can be derived from the kinetic theory through the moment technique. In particular, two species of moments can be introduced [33]: the momentum-

like F moments and the energy-like G moments, defined as

$$F = m\int_{\mathbb{R}^3}\int_0^{+\infty} f\varphi(I)dI\,d\mathbf{c}, \quad F_{i_1 i_2 \dots i_h} = m\int_{\mathbb{R}^3}\int_0^{+\infty} f c_{i_1}c_{i_2}\dots c_{i_h}\varphi(I)dId\mathbf{c},$$
$$G_{ss} = m\int_{\mathbb{R}^3}\int_0^{+\infty} f\left(c^2+\frac{2I}{m}\right)\varphi(I)dId\mathbf{c},\ G_{ssi_1\dots i_h} = m\int_{\mathbb{R}^3}\int_0^{+\infty} f\left(c^2+\frac{2I}{m}\right)c_{i_1}c_{i_2}\dots c_{i_h}\varphi(I)dId\mathbf{c},$$

if m denotes the mass of the gas molecule and the indexes $h \in \mathbb{N}\backslash\{0\}$, $i_h = 1,2,3$. Moreover, for a polytropic gas with internal energy $\varepsilon = Dk_BT/(2m)$ (if k_B denotes the Boltzmann constant, T the temperature and D the degrees of freedom of a gas molecule) the wheighting function is given by $\varphi = I^{(D-5)/2}$.

In this way it is possible to derive from (8) a double infinite hierarchy of balance laws [33]:

$$\begin{array}{ll}
\partial_t F + \partial_j F_j = 0, & \\
\quad\swarrow & \\
\partial_t F_{i_1} + \partial_j F_{ji_1} = 0, & \\
\quad\swarrow & \\
\partial_t F_{i_1 i_2} + \partial_j F_{ji_1 i_2} = P_{i_1 i_2}, & \partial_t G_{ss} + \partial_j G_{ssj} = 0, \\
\quad\swarrow & \quad\swarrow \\
\partial_t F_{i_1 i_2 i_3} + \partial_j F_{ji_1 i_2 i_3} = P_{i_1 i_2 i_3}, & \partial_t G_{ssi_1} + \partial_j G_{ssji_1} = Q_{ssi_1}, \\
\vdots & \vdots \\
\partial_t F_{i_1 i_2 \dots i_h} + \partial_j F_{ji_1 i_2 \dots i_h} = P_{i_1 i_2 \dots i_h}, & \partial_t G_{ssi_1 i_2 \dots i_h} + \partial_j G_{ssji_1 i_2 \dots i_h} = Q_{ssi_1 i_2 \dots i_h}. \\
\vdots & \vdots
\end{array} \tag{9}$$

where $P_{i_1\dots i_h}$ and $Q_{ssi_1\dots i_h}$ denotes the production components obtained from the collisional term of the Boltzmann equation, through the moment technique. For the sake of brevity, from now on repeated indexes imply their sum, so that for example $\sum_{j=1}^3$ is omitted in (9).

It is easily verified that the first two equations of the momentum-hierarchy and the first scalar equation of the energy-hierarchy coincide with the usual conservation laws of mass, momentum and energy. Both hierarchies (9) exhibit a peculiar mathematical structure since the density component of one equation coincides with the flux component of the previous one [33]. To deduce a finite

set of PDEs, the infinite set (9) is truncated at some truncation indexes (N for the F-hierarchy and M for the G-hierarchy) and one expresses the last fluxes and production terms as functions of the independent field variables referring to the Maximum Entropy Principle (closure of the system) [33]. The resulting set of equations proves to be of hyperbolic type, and for a suitable choice of the independent field variables (the so called *main field* [33, 34]), it could be written in symmetric hyperbolic form with a convex entropy, guaranteeing the well-posedness of the Cauchy problem.

The truncated and closed system is then commonly approximated by a Taylor expansion in the neighbourhood of a local equilibrium. In the present work we will consider a linearized theory with respect to the non-equilibrium variables [33] denoted by $\mathrm{ET}^1_{n,P}$, where the '1' recalls the first order Taylor approximation, n indicates the number of scalar equations of the model and the letter P is associated with a polyatomic gas.

For the sake of brevity, the density, the flux and the productions components can be written as

$$\mathbf{F} = (F, F_{i_1}, F_{i_1 i_2}, \dots F_{i_1 i_2 \dots i_N})^T, \qquad \mathbf{F}^j = (F_j, F_{j i_1}, F_{j i_1 i_2}, \dots F_{j i_1 i_2 \dots i_N})^T,$$
$$\mathbf{G}_{ss} = (G_{ss}, G_{ssi_1}, G_{ssi_1 i_2}, \dots G_{ssi_1 i_2 \dots i_M})^T, \quad \mathbf{G}^j_{ss} = (G_{ssj}, G_{ssj i_1}, G_{ssj i_1 i_2}, \dots G_{ssj i_1 i_2 \dots i_M})^T,$$
$$\mathbf{P} = (0, 0_{i_1}, P_{i_1 i_2}, \dots P_{i_1 i_2 \dots i_N})^T, \qquad \mathbf{Q} = (0, Q_{ssi_1}, Q_{ssi_1 i_2}, \dots Q_{ssi_1 i_2 \dots i_M}),$$

and the PDEs summerized in the formulas:

$$\partial_t \mathbf{F} + \partial_j \mathbf{F}^j = \mathbf{P}, \quad \partial_t \mathbf{G}_{ss} + \partial_j \mathbf{G}^j_{ss} = \mathbf{Q}. \tag{10}$$

If $\mathbf{u}$ denotes the vector of the field variables and if the dependence of only a scalar space variable $z = z_1$ is assumed, system (10) reduces to

$$\mathbf{C}(\mathbf{u})\partial_t \mathbf{u} + \mathbf{D}(\mathbf{u})\partial_z \mathbf{u} = \mathbf{T}', \quad \text{with} \quad \mathbf{C}(\mathbf{u}) = \partial_{\mathbf{u}}(\mathbf{F}, \mathbf{G}_{ss}), \quad \mathbf{D}(\mathbf{u}) = \partial_{\mathbf{u}} = \partial_{\mathbf{u}}(\mathbf{F}^1, \mathbf{G}^1_{ss}), \tag{11}$$

where $\mathbf{T}' = (\mathbf{P}, \mathbf{Q})$ and $\partial_z = \partial \cdot / \partial z$. A further simplification in the equation structure is developed through the introduction of the material derivative $\overset{\bullet}{*} = \frac{\partial *}{\partial t} + v \frac{\partial *}{\partial z}$ where v is the gas velocity along

the z direction; hence, (11) becomes

$$\partial_t \mathbf{u} + \mathbf{B}(\mathbf{u})\partial_z \mathbf{u} = \mathbf{T} \qquad \Longrightarrow \qquad \overset{\bullet}{\mathbf{u}} + \mathbf{A}(\mathbf{u})\partial_z \mathbf{u} = \mathbf{T}, \tag{12}$$

where $\mathbf{B} = \mathbf{C}^{-1}\mathbf{D}$, $\mathbf{T} = \mathbf{C}^{-1}\mathbf{T}'$ and $\mathbf{A} = \mathbf{B} - v\mathbf{I}$, if $\mathbf{I}$ indicates an identity matrix of the same size as the square matrix $\mathbf{A}$. The characteristic velocities associated with the equation system are obviously the eigenvalues λ of $\mathbf{B}$, and there exists a relation between the eigenvalues Λ of $\mathbf{A}$ and those of $\mathbf{B}$: $\lambda = \Lambda + v$.

Here we restrict our analysis to ideal polyatomic gases, so that the equilibrium gas pressure is $p = k_B \rho T/m$ (ρ is the mass density) and the specific heat at constant volume is $c_v = k_B D/2m$. The parameter D is defined as the sum of translational and internal degrees of freedom of the molecules: in general $D \geq 3$, while $D = 3$ represents the case of a monatomic gas.

One of the most popular theories derived through the RET procedures is the 14-moment system $\mathrm{ET}^1_{14,P}$, in which together with mass density ρ, velocity $\mathbf{v} = (v_1, v_2, v_3)$ and equilibrium pressure p, also the deviatoric part of the viscous stress tensor $\sigma_{\langle ij \rangle}$, the dynamic pressure Π and the heat flux $\mathbf{q} = (q_1, q_2, q_3)$ are treated as independent field variables:

$$\begin{aligned}
&\mathbf{F} = (F, F_k, F_{kl})\,, \qquad \mathbf{F}^j = (F_j, F_{jk}, F_{jkl})\,, \qquad \mathbf{G}_{ss} = (G_{ss}, G_{ssk})\,, \qquad \mathbf{G}^j_{ss} = (G_{ssj}, G_{ssjk})\,,\\
&\text{with} \quad F = \rho, \quad F_k = \rho v_k, \quad F_{kl} = \rho v_k v_l + (p + \Pi)\delta_{kl} - \sigma_{\langle kl \rangle},\\
&F_{jkl} = \rho v_j v_k v_l + (p + \Pi)(v_j \delta_{kl} + v_k \delta_{jl} + v_l \delta_{jk}) - \sigma_{\langle jk \rangle} v_l - \sigma_{\langle kl \rangle} v_j - \sigma_{\langle jl \rangle} v_k +\\
&\qquad + \frac{2}{D+2}(q_j \delta_{kl} + q_k \delta_{jl} + q_l \delta_{jk}),
\end{aligned}$$

$$\begin{aligned}
&G_{ss} = \rho |v|^2 + 2\rho\epsilon, \quad G_{ssk} = \rho |v|^2 v_k + 2(\rho\epsilon + p + \Pi) v_k - 2\sigma_{\langle ks \rangle} v_s + 2q_k),\\
&G_{ssjk} = \rho |v|^2 v_j v_k + 2\rho\epsilon v_j v_k + (p + \Pi)(|v|^2 \delta_{jk} + 4 v_j v_k) - \sigma_{\langle jk \rangle} |v|^2 - 2\sigma_{\langle jh \rangle} v_k v_h -\\
&\qquad - 2\sigma_{\langle kh \rangle} v_j v_h + \frac{2}{D+2}\left(2q_h v_h \delta_{jk} + (D+4)(q_j v_k + q_k v_j)\right) +\\
&\qquad + \frac{k_B T}{m}[(D+2)p + (D+4)\Pi]\delta_{jk} - \frac{k_B T}{m}(D+4)\sigma_{\langle jk \rangle}, \quad \text{if } i, j, k, l, s = 1, 2, 3.
\end{aligned} \tag{13}$$

We remark that the well-known Grad's model can be derived from $\mathrm{ET}^1_{14,P}$ in the limit $D \to 3$, neglecting the dynamic pressure.

IV.A. RET balance laws in an oscillating cylindrical domain

In the next Sections we are going to study the behaviour of a gas inside a shrinking cylindrical bubble. To this aim it is convenient to rewrite the previous equations in cylindrical coordinates and then to account for the domain oscillations introducing a suitable transformation of the space and time variables. Firstly, we will refer to cylindrical coordinates (r, ϑ, x_3) ($\vartheta \in [0, 2\pi[$) and instead of the usual contra- or co-variant components of vectors and tensors, we will employ the physical components [46], so that, for example

$$\bar{q}^i = \sqrt{g_{\underline{ii}}}q^i, \quad \bar{\sigma}^{\langle ij\rangle} = \sqrt{g_{\underline{ii}}g_{\underline{jj}}}\sigma^{\langle ij\rangle}, \quad \text{with} \quad i,j,=1,2,3,$$

where the repeated underlined indexes are not summed and g_{ij} denotes the (ij) component of the metric tensor (g_{ij} is a diagonal tensor with $g_{11} = g_{33} = 1$, $g_{22} = r^2$ in the cylindrical case). The bar denotes here the physical component, but in the following we will omit such a symbol for the sake of brevity. We assume that the gas velocity and the heat flux are parallel to the radial direction ($\mathbf{v} = (v, 0, 0)$, $\mathbf{q} = (q, 0, 0)$ with $v = v^1$ and $q = q^1$), and, moreover, $\sigma^{\langle ij\rangle} = 0$ when $i \neq j$. We recall that, by definition, $\sigma^{\langle ll\rangle} = 0$, so in cylindrical symmetry the field vector should include $\sigma^{\langle 22\rangle}$, while $\sigma^{\langle 33\rangle} = -\sigma^{\langle 11\rangle} - \sigma^{\langle 22\rangle}$. The equation system turns out to be

$$\begin{aligned}
&\overset{\bullet}{\rho} + \rho\ \partial_r v = \mathcal{P}_1\\
&\overset{\bullet}{v} - \frac{1}{\rho}\partial_r\sigma^{\langle 11\rangle} + \frac{1}{\rho}\partial_r\Pi + \frac{1}{\rho}\partial_r p = \mathcal{P}_2\\
&\overset{\bullet}{\sigma}^{\langle 11\rangle} + \frac{7\sigma^{\langle 11\rangle} - 4(p+\Pi)}{3}\partial_r v - \frac{8}{3(D+2)}\partial_r q = \mathcal{P}_3\\
&\overset{\bullet}{\sigma}^{\langle 22\rangle} + \left[\frac{2}{3}(p + \Pi - \sigma^{\langle 11\rangle}) + \sigma^{\langle 22\rangle}\right]\partial_r v + \frac{4}{3(D+2)}\partial_r q = \mathcal{P}_4\\
&\overset{\bullet}{\Pi} + [\Pi - \frac{2(D-3)(\sigma^{11} - p)}{3D}]\partial_r v + \frac{4(D-3)}{3D(D+2)}\partial_r q = \mathcal{P}_5\\
&\overset{\bullet}{p} + [p + \frac{2(p-\sigma^{11})}{D}]\partial_r v + \frac{2}{D}\partial_r q = \mathcal{P}_6\\
&\overset{\bullet}{q} + \frac{p}{2\rho^2}[2\sigma^{11} - (D+2)(p-\sigma^{11})]\partial_r\rho + \frac{2(D+5)q}{D+2}\partial_r v - \frac{\sigma^{11}+p}{\rho}(\partial_r\sigma^{\langle 11\rangle} - \partial_r\Pi) +\\
&+ \frac{(D+2)(p-\sigma^{11})}{2\rho}\partial_r p = \mathcal{P}_7
\end{aligned} \tag{14}$$

where

$$
\begin{aligned}
\mathcal{P}_1 &= -\frac{\rho v}{r}, \qquad \mathcal{P}_2 = \frac{(\sigma^{\langle 11\rangle} - \sigma^{\langle 22\rangle})}{r\rho}, \qquad \mathcal{P}_6 = -2\frac{q}{Dr} - 2\frac{(p+\Pi-\sigma^{\langle 22\rangle})v}{Dr} - \frac{pv}{r},\\
\mathcal{P}_3 &= -\frac{\sigma^{\langle 11\rangle}}{\tau_\sigma} - \frac{4q}{3(D+2)r} - \frac{v}{3r}[2(p+\Pi) + 3\sigma^{\langle 11\rangle} - 2\sigma^{\langle 22\rangle}],\\
\mathcal{P}_4 &= -\frac{\sigma^{\langle 22\rangle}}{\tau_\sigma} + \frac{8q}{3(D+2)r} - \frac{v}{3r}[7\sigma^{\langle 22\rangle} - 4p - 4\Pi],\\
\mathcal{P}_5 &= -\frac{\Pi}{\tau_\Pi} - \frac{4(D-3)q}{3D(D+2)r} - \frac{6(\sigma^{\langle 22\rangle} - p - \Pi) + D(-2\sigma^{\langle 22\rangle} + 5\Pi + 2p)v}{3Dr},\\
\mathcal{P}_7 &= -\frac{q}{\tau_q} - \frac{1}{r}\left[\frac{(\sigma^{\langle 22\rangle} - \sigma^{\langle 11\rangle})(p+\sigma^{11})}{\rho} + \frac{(D+4)qv}{D+2}\right].
\end{aligned}
\tag{15}
$$

For the relaxation times of dynamic pressure, stress tensor and heat flux, (denoted by τ_Π, τ_σ and τ_q) the following relations hold, if μ_b is the bulk viscosity, ν the shear viscosity and κ the heat conductivity of the gas [33, 35]:

$$
\tau_\sigma = \frac{\nu}{p}, \quad \tau_q = \frac{2\kappa m}{5k_B p}, \quad \tau_\Pi = \frac{3D\mu_b}{2(D-3)p}. \tag{16}
$$

In addition, in (14) and (15) we introduce to the (11)-component of the viscous tensor $\sigma^{11} = \sigma^{\langle 11\rangle} - \Pi$ in order to compress some formulas.

The bubble radius varies in time and so does the domain in which the AWs propagate. To simplify the calculations in the case of an oscillating cylindrical domain with a time variable radius $R = R(t)$, we consider a transformation from the usual time-space variables $\{t, r\}$ (with r radial coordinate inside the bubble $r \in [0, R(t)]$) to the more comfortable $\{t', x\}$ if $t' = t$ and $x = r/R(t)$ with $x \in [0, 1]$. Therefore, the PDE system (5) is transformed as following

$$
\partial_t \mathbf{u} + \mathbf{B}\partial_r \mathbf{u} = \mathbf{T} \quad \Rightarrow \quad \partial_t \mathbf{u} + \frac{1}{R(t)}\left[\mathbf{B} - x\dot{R}\,\mathbf{I}\right]\partial_x \mathbf{u} = \mathbf{T}. \tag{17}
$$

It is easily proved that the characteristic velocities (λ') of the transformed system $(17)_2$ are related

to those (λ) of the initial system $(17)_1$ by $\lambda' = \left(\lambda - x\dot{R}\right)/R(t)$. System (14) can be rewritten as

$$
\begin{aligned}
&\partial_t\rho + \frac{v - x\dot{R}}{R}\partial_x\rho + \frac{\rho}{R}\partial_x v = -\frac{\rho v}{Rx},\\
&\partial_t v + \frac{v - x\dot{R}}{R}\partial_x v + \frac{1}{\rho R}\partial_x(p + \Pi - \sigma^{\langle 11\rangle}) = \frac{\sigma^{\langle 11\rangle} - \sigma^{\langle 22\rangle}}{\rho R x},\\
&\partial_t\sigma^{\langle 11\rangle} + \frac{7\sigma^{\langle 11\rangle} - 4(p+\Pi)}{3R}\partial_x v + \frac{v - x\dot{R}}{R}\partial_x\sigma^{\langle 11\rangle} - \frac{8}{3(D+2)}\partial_x q =\\
&= -\frac{\sigma^{\langle 11\rangle}}{\tau_\sigma} - \frac{4q}{3(D+2)Rx} - \frac{v}{3Rx}(2(p+\Pi) + 3\sigma^{\langle 11\rangle} - 2\sigma^{\langle 22\rangle}),\\
&\partial_t\sigma^{\langle 22\rangle} + \frac{1}{R}[\frac{2}{3}(p + \Pi - \sigma^{\langle 11\rangle}) + \sigma^{\langle 22\rangle}]\partial_x v + \frac{v - x\dot{R}}{R}\partial_x\sigma^{\langle 22\rangle} + \frac{4}{3(D+2)R}\partial_x q =\\
&- \frac{\sigma^{\langle 22\rangle}}{\tau_\sigma} + \frac{8q}{3(D+2)Rx} - \frac{v}{3Rx}[7\sigma^{\langle 22\rangle} - 4(p+\Pi)],\\
&\partial_t\Pi + \frac{2(D-3)(p - \sigma^{\langle 11\rangle}) + (5D-6)\Pi}{3DR}\partial_x v + \frac{v - x\dot{R}}{R}\partial_x\Pi + \frac{4(D-3)}{3D(D+2)R}\partial_x q =\\
&= -\frac{\Pi}{\tau_\Pi} - \frac{4(D-3)q}{3D(D+2)Rx} - \frac{2(D-3)(p + \Pi - \sigma^{\langle 22\rangle}) + 3D\Pi}{3DRx}v,\\
&\partial_t p + \frac{(D+2)p - 2\sigma^{11}}{DR}\partial_x v + \frac{v - x\dot{R}}{R}\partial_x p + \frac{2}{DR}\partial_x q = -\frac{2q}{DRx} - \frac{((D+2)p + 2\Pi - 2\sigma^{\langle 22\rangle})v}{DRx},\\
&\partial_t q + \frac{p}{2\rho^2 R}[2\sigma^{11} - (D+2)(p - \sigma^{11})]\partial_x\rho + \frac{2(D+5)q}{(D+2)R}\partial_x v - \frac{\sigma^{11} + p}{\rho R}(\partial_x\sigma^{\langle 11\rangle} - \partial_x\Pi) +\\
&+ \frac{(D+2)(p - \sigma^{11})}{2\rho R}\partial_x p + \frac{v - x\dot{R}}{R}\partial_x q = -\frac{q}{\tau_q} - \frac{1}{Rx}\Big[\frac{(\sigma^{\langle 22\rangle} - \sigma^{\langle 11\rangle})(p + \sigma^{11})}{\rho} + \frac{(D+4)qv}{D+2}\Big].
\end{aligned}
\tag{18}
$$

Neglecting the contribution of heat flux and stress tensor, the previous set of equations reduces to the $\mathrm{ET}_{6,P}$ model, where the only non-equilibrium variable taken into account is the dynamic pressure [33]. Such a system is commonly employed when τ_Π is much greater than τ_σ and τ_q (see [33] and the references therein). Under the previous assumptions, system (18) transforms in

$$
\begin{aligned}
&\partial_t\rho + \frac{v - x\dot{R}}{R}\partial_x\rho + \frac{\rho}{R}\partial_x v = -\frac{\rho v}{Rx},\\
&\partial_t v + \frac{v - x\dot{R}}{R}\partial_x v + \frac{1}{\rho R}\partial_x(p + \Pi) = 0,\\
&\partial_t\Pi + \frac{2(D-3)p + (5D-6)\Pi}{3DR}\partial_x v + \frac{v - x\dot{R}}{R}\partial_x\Pi = -\frac{(2(D-3)p + (5D-6)\Pi)v}{3DRx} - \frac{\Pi}{\tau_\Pi},\\
&\partial_t p + \frac{(D+2)p + 2\Pi}{DR}\partial_x v + \frac{v - x\dot{R}}{R}\partial_x p = -\frac{(D+2)pv}{DRx} - \frac{2\Pi v}{DRx}.
\end{aligned}
\tag{19}
$$

V. ACCELERATION WAVES IN A CYLINDRICAL BUBBLE MODELLED BY RET THEORIES

In what follows the AW propagation is modelled referring to $\mathrm{ET}^{1}_{14,P}$ and $\mathrm{ET}_{6,P}$ equations. We restrict the analysis to a linear time-dependence of the bubble radius

$$R(t) = R_0(1 + \mu t), \tag{20}$$

where R_0 is the initial bubble radius, and $\mu < 0$ represents the case of a linear contraction of the bubble. Due to this assumption, the description of the unperturbed fields will be valid only for small time intervals, accordingly with a fast AW propagation. Concerning the unperturbed field vector $\mathbf{u}_u$ we introduce also an adiabatic hypothesis ($q_u = 0$) and the natural boundary conditions: $v_u = 0$ in $x = 0$ and $v_u = \dot{R}$ in $x = 1$. In this manner, the requirement of a linear dependence of v_u on x implies $v_u = x\dot{R}$. Finally, neglecting the bubble wall acceleration it is possible to require the space uniformity of unperturbed pressure, mass density and dynamic pressure. The procedure is an extension of the results in [36].

V.A. $\mathrm{ET}_{6,P}$ theory

If the AW propagating from the boundary to the centre of the bubble is described by a six-moment RET theory (19), its characteristic velocity turns out to be $\tilde{\lambda} = -\frac{1}{R}\sqrt{\frac{5(p+\Pi)}{3\rho}}$ (independent on D [33]) and the wave front equation reads $\frac{dx}{dt} = \tilde{\lambda}_u$ with $x(0) = 1$, since the AW propagates starting from the bubble wall. Considering the previous assumptions about the unperturbed field vector $\mathbf{u}_u = (\tilde{\rho}_u, \tilde{v}_u, \tilde{\Pi}_u, \tilde{p}_u)$, it is easily shown that only a solution with non-vanishing dynamic pressure is compatible with (19). A similar result was already deduced in spherical symmetry for the RET models [36]. Furthermore, it is easly verified that

$$\begin{aligned}
&\tilde{\rho}_u = \rho_0(R_0/R)^2,\\
&\frac{d\tilde{\Pi}_u}{dt} = -\frac{4(D-3)\tilde{p}_u\dot{R}}{3DR} - \frac{2(5D-6)\tilde{\Pi}_u\dot{R}}{3DR} - \frac{\tilde{\Pi}_u}{\tau_\Pi},\\
&\frac{d\tilde{p}_u}{dt} = -\frac{2(D+2)\tilde{p}_u\dot{R}}{DR} - \frac{4\tilde{\Pi}_u\dot{R}}{DR},
\end{aligned} \tag{21}$$

where the previous ODE equations should be equipped with the initial conditions $\tilde{p}_u(0) = p_0$ and $\tilde{\Pi}_u(0) = \Pi_0$. After some calculations the Bernoulli's coefficients are completely determined

$$a = -\frac{4}{3\tilde{\lambda}_u R}, \quad b = \frac{\tilde{\lambda}_u}{2x} + \frac{11\dot{R}}{6R} + \frac{4(D-3)\tilde{p}_u + (5D-12)\tilde{\Pi}_u}{20D(\tilde{p}_u + \tilde{\Pi}_u)\tau_\Pi}, \tag{22}$$

where x corresponds to the instantaneous position of the wavefront. Functions g_1 and g_2 in (6) could be easily evaluated through a numerical integration, starting from the numerical solution of the two ODEs in (21).

V.B. $\mathbf{ET}^1_{14,P}$ theory

In the case of a 14-moment model, the calculations become more complicated and so, in this work, we restrict our study to the case $D = 5$, similar results could be obtained fixing different values for D. Concerning the unperturbed adiabatic solution, as already said, we assume that $\hat{q}_u = 0$, $\hat{v}_u = x\dot{R}$. Equations (18) in cylindrical symmetry require not only a non-zero dynamic pressure (as for spherical geometry [36,47] and for ET_6, P theory), but also a non-zero stress tensor, while it is natural to impose $\hat{\sigma}_u^{\langle 11\rangle} = \hat{\sigma}_u^{\langle 22\rangle} = \hat{s}_u$. This fact is in accordance with the Navier-Stokes (NS) approximation, since for a cylindrical gas bubble described by the Navier-Stokes theory it must hold

$$\Pi_{NS} = -2\frac{\mu_b \dot{R}}{R}, \qquad \sigma_{NS}^{\langle 11\rangle} = -\frac{2}{3}\frac{\nu\dot{R}}{R}. \tag{23}$$

Through compatibility conditions it could be easily deduced that $\partial_x \hat{\rho}_u = \partial_x \hat{p}_u = \partial_x \hat{\Pi}_u = \partial_x \hat{s}_u = 0$. Together with relation $\hat{\rho}_u = \rho_0 (R_0/R)^2$ (as in ET_6, P), the following ODEs hold for the remaining unperturbed field components

$$\begin{aligned}
\frac{d\hat{s}_u}{dt} &= \frac{2(\hat{p}_u + \hat{\Pi}_u - 4\hat{s}_u)\dot{R}}{3R} - \frac{\hat{s}_u}{\tau_\sigma}, \\
\frac{d\hat{\Pi}_u}{dt} &= -\frac{2(4\hat{p}_u + 19\hat{\Pi}_u - 4\hat{s}_u)\dot{R}}{15R} - \frac{\hat{\Pi}_u}{\tau_\Pi}, \\
\frac{d\hat{p}_u}{dt} &= -\frac{2(7\hat{p}_u + 2\hat{\Pi}_u - 2\hat{s}_u)\dot{R}}{5R}.
\end{aligned} \tag{24}$$

The negative characteristic speeds of the AW propagating into an unperturbed solution

depend on D and when $D=5$ they turn out to be

$$\hat{\lambda}_u^{(1,2)} = -\frac{1}{R}\sqrt{\frac{85\hat{p}_u - 69\hat{s}_u \pm \sqrt{3550\hat{p}_u^2 - 4380\hat{p}_u\hat{s}_u + 36\hat{s}_u^2}}{35\hat{\rho}_u}}. \tag{25}$$

Moreover, the equation of the wave front presents the usual form $dx/dt = \hat{\lambda}_u$. Bernoulli's coeffcients can be determined after some calculations:

$$\begin{aligned}
a &= -\frac{\hat{\lambda}_u^2\hat{\rho}_u R^2\nu_4 + \nu_5}{5\hat{\lambda}_u^3\hat{\rho}_u R^3\delta_1}, \qquad b = \frac{\lambda}{2x} + b_{\dot{R}}\frac{\dot{R}}{R} + \frac{b_\sigma}{\tau_\sigma} + \frac{b_q}{\tau_q} + \frac{b_\Pi}{\tau_\Pi},\\
b_{\dot{R}} &= \frac{3(\hat{\rho}_u\hat{\lambda}_u^2 R^2\nu_1 - 5\nu_2\nu_3)}{25\hat{\lambda}_u^2\hat{\rho}_u R^2\delta_1\delta_2^2}, \quad b_q = \frac{7\hat{\lambda}_u^2\hat{\rho}_u R^2(15\hat{p}_u^2 - 14\hat{p}_u\hat{s}_u - 6\hat{s}_u^2))}{4\delta_2},\\
b_\sigma &= \frac{7\hat{\lambda}_u^2\hat{\rho}_u R^2(5\nu_7 + 3(\hat{\Pi}_u + \hat{s}_u)\mu_5) - \nu_3(5\nu_6 + 3(\hat{\Pi}_u + \hat{s}_u)\mu_4)}{6\hat{\lambda}_u^2\hat{\rho}_u R^2\delta_1\delta_2},\\
b_\Pi &= \frac{7\hat{\lambda}_u^2\hat{\rho}_u R^2(\nu_7 - 3\hat{\Pi}_u\mu_5) - \nu_3(\nu_6 - 3\hat{\Pi}_u\mu_4)}{6\hat{\lambda}_u^2\hat{\rho}_u R^2\delta_1\delta_2},
\end{aligned} \tag{26}$$

where x coincide with the position of the wave front and

$$\begin{aligned}
&\delta_1 = (35\lambda^2\hat{\rho}_u R^2 - 65\hat{p}_u + 33s)(35\lambda^2\hat{\rho}_u R^2 - 85\hat{p}_u + 69\hat{s}_u),\\
&\delta_2 = \lambda^2\hat{\rho}_u R^2(175\hat{p}_u^2 - 294\hat{p}_u\hat{s}_u + 84\hat{s}_u^2) + (-70p^3 + 266\hat{p}_u^2\hat{s}_u - 342\hat{p}_u\hat{s}_u^2 + 162\hat{s}_u^3),\\
&\nu_1 = 43584933125\hat{p}_u^8 - 266040784375\hat{p}_u^7\hat{s}_u + 661256633425\hat{p}_u^6\hat{s}_u^2 - 850946456275\hat{p}_u^5\hat{s}_u^3 +\\
&+ 591162202044\hat{p}_u^4\hat{s}_u^4 - 204964083456\hat{p}_u^3\hat{s}_u^5 + 24819240204\hat{p}_u^2\hat{s}_u^6 + 1252289484\hat{p}_u\hat{s}_u^7 - 108094176\hat{s}_u^8,\\
&\nu_2 = 902412625\hat{p}_u^7 - 4851681000\hat{p}_u^6\hat{s}_u + 10228203095\hat{p}_u^5\hat{s}_u^2 - 10498223424\hat{p}_u^4\hat{s}_u^3 +\\
&+ 5177323296\hat{p}_u^3\hat{s}_u^4 - 936327744\hat{p}_u^2\hat{s}_u^5 - 25847964\hat{p}_u\hat{s}_u^6 + 4498416\hat{s}_u^7,\\
&\nu_3 = 7\hat{p}_u^2 - 14\hat{p}_u\hat{s}_u + 9\hat{s}_u^2,\\
&\nu_4 = 7(10605\hat{p}_u^2 - 15074\hat{p}_u\hat{s}_u + 2364\hat{s}_u^2),\ \nu_5 = -15(2527\hat{p}_u^3 - 7301\hat{p}_u^2\hat{s}_u + 7418\hat{p}_u\hat{s}_u^2 - 2724\hat{s}_u^3),\\
&\nu_6 = 28(3400\hat{p}_u^4 - 10010\hat{p}_u^3\hat{s}_u + 9237\hat{p}_u^2\hat{s}_u^2 - 2574\hat{p}_u\hat{s}_u^3 + 54\hat{s}_u^4),\\
&\nu_7 = 4(32875\hat{p}_u^5 - 120985\hat{p}_u^4\hat{s}_u + 157681\hat{p}_u^3\hat{s}_u^2 - 84057\hat{p}_u^2\hat{s}_u^3 + 14976\hat{p}_u\hat{s}_u^4 - 270\hat{s}_u^5),\\
&\mu_5 = 80275\hat{p}_u^4 - 84245\hat{p}_u^3\hat{s}_u - 128517\hat{p}_u^2\hat{s}_u^2 + 143064\hat{p}_u\hat{s}_u^3 - 15822\hat{s}_u^4,\\
&\mu_4 = 51850\hat{p}_u^3 - 12885\hat{p}_u^2\hat{s}_u - 103770\hat{p}_u\hat{s}_u^2 + 23706\hat{s}_u^3.
\end{aligned} \tag{27}$$

Through a numerical integration of (24), wave front equation and (26), g_1 and g_2 are evaluated as functions of time.

VI. SOME PHYSICAL EXAMPLES

The determination of the unperturbed fields $\mathbf{u}_u$ is the first step into the study of AWs. Referring to Section IV, the unperturbed variables will be determined integrating numerically (24) or (21). As already remarked, the 6-moment theory is incompatible with a vanishing dynamic pressure, while the 14-moment model impose also the presence of a non-zero stress tensor, in complete agreement with the Navier-Stokes approximation (23). The values of Π_u and $\sigma_u^{\langle 11\rangle}$ should be related to the velocity of the bubble wall, and their contribution could become relevant when $R < R_M$ and $|\dot{R}| >> 0$.

In order to obtain semi-analytical results concerning the AW evolution, we have introduced some simplifying assumptions, summarized in the following.

- The molecular degrees of freedom is fixed at a constant value; we have chosen $D = 5$, since it is rather realistic for many common diatomic molecules at room temperature, although not valid for all gases.

- Heat conductivity, shear and bulk viscosity are modelled as constant quantities, as well.

- We have imposed the adiabaticity of the system (so that $q_u = 0$) and a linear behaviour of the bubble radius ($\dot{R} = \dot{R}_0 = constant$) during the wave propagation. Both assumptions are compatible with the small size of the propagation time interval. As a matter of fact, the AW presents a very high wave speed, if compared with the bubble wall velocity: the contraction of the cylindrical bubble remains always subsonic and no violent phenomena were observed in the experiments [16–19].

- The gas velocity is assumed to be linear in space: $v_u = x\dot{R}_0$.

- t_* indicates the propagation time of the AW that starts from the bubble wall and reaches the cylinder axis. As already remarked in [36], it is physically meaningless to imagine the wave front reaching $x = 0$. For an incoming AW, the wave front should stop at a distance of at least the molecular kinetic diameter, δ, ($x(t'_*) = \delta/R$) and bounce back. However, t_*

is very close to t'_* and in the cylindrical case the function g_2 in (6) does not diverge when $x(t) \to 0$ [24, 36], in contrast with the spherical bubble case [24, 36, 43]. So, for the sake of simplicity, from now on we will consider t_* in spite of t'_*.

- $R_0 = R(0)$ and $\dot{R}_0 = \dot{R}(0)$ represents respectively the values of the bubble radius and the bubble wall velocity, if $t = 0$ is the instant in which the AW is generated. Here, $R_0 = 43\mu$m and $R_\infty = 0.5$mm as in [16].

- The integration of equations (24) requires the prescription of the initial values of equilibrium pressure p_0, dynamic pressure Π_0 and stress tensor $\sigma_0^{\langle 11\rangle}$. The initial pressure should be fixed as $p_0 = p_M(R_M/R_0)^\beta$ where p_M is the gas equilibrium pressure at R_M, while $\beta = 2$ for an isothermal bubble shrinkage, and $\beta = 2(D+2)/D = 14/5$ in an adiabatic bubble contraction. It is natural to refer to the Navier-Stokes approximation (23) to choose Π_0 and $\sigma_0^{\langle 11\rangle}$.

- The solution of the system derived from to the RET theory with 6 moments follows the same ideas, except for the stress tensor that is neglected by the model.

Due to the small value of t_*, no significant differences can be observed concerning the unperturbed equilibrium pressure and the dynamic pressure described by the $\mathrm{ET}_{6,P}$ and $\mathrm{ET}^1_{14,P}$. An illustrative comparison of Π_u and $\sigma_u^{\langle 11\rangle}$ predicted by (24) for different gases is presented in Figure 2. The physical parameters of the gases were fixed referring to [48]. We remark that the case of carbon dioxide was studied under the assumption $\mu_b/\nu = 50$, but very different values of this ratio are reported in the literature (see for instance [49–52]). It is easy to understand that higher values of this ratio would give rise to values of the dynamic pressure (and consequently of the total gas pressure) not compatible with approximation (4). This question should be further studied taking into account the coupling between equation (3) and the gas dynamics PDEs.

Concerning the AWs, we refer to some physical examples and determine here the critical values $\mathcal{A}_{cr}$ of the scalar amplitude, predicted by RET theory with 14 or 6 moments, corresponding to the fastest wave. In Figure 3 we present the qualitative behaviour of g_2 as a function of time t/t_* for different physical parameters in the case of a bubble filled with water vapour. In particular, *case 1*: $\mathrm{p}_0 = 10^3$Pa, $R_0 \simeq 43\mu$m, $\dot{R}_0 \simeq -0.0062$m/s; *case 2*: $p_0 \simeq 1.12 \times 10^4$Pa, $R_0 \simeq 18.1\mu$m, $\dot{R} \simeq -11.8$m/s; *case 3*: $p_0 \simeq 8.07 \times 10^5$Pa, $R_0 \simeq 3.94\mu$m, $\dot{R} \simeq -49.4$m/s; *case 4*: $p_0 \simeq 10^2$Pa, $R_0 \simeq 43\mu$m, $\dot{R} \simeq -0.0062$m/s; *case 5*: $p_0 \simeq 1.12 \times 10^3$Pa, $R_0 \simeq 18.1\mu$m, $\dot{R} \simeq -11.8$m/s; where

(a) **(b)**

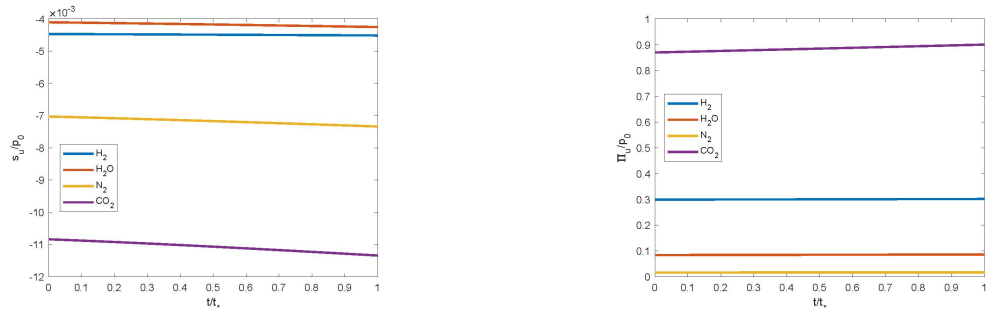

Fig. 2. The behaviour of $s_u = \sigma_u^{\langle 11 \rangle}$ (a) and Π_u (b) for different gases when $p_0 \simeq 1.12 \times 10^3$Pa, $R_0 \simeq 18.1\mu$m and $\dot{R}_0 \simeq -11.8$m/s; for CO_2 it is assumed that $\mu_b/\nu = 50$.

$c_0 = \sqrt{k_B T_0/m}$ if $T(0) = T_0$.

It is reasonable to assume that a possible initial scalar amplitude of the AW shares the same magnitude order as the bubble wall acceleration $\mathcal{A}(0) \simeq \ddot{R}$. Figure 4 contains the comparison of $\ddot{R}$ and $\mathcal{A}_{cr}$.

AWs could transform into a shock wave only for negative initial scalar amplitude $\mathcal{A}(0) \leq \mathcal{A}_{cr}$ ($g_2(t) \geq 0$ for incoming waves), from Figures 4 one can easily conclude that no shock wave is observable in cylindrical bubble, at least in the range of physical conditions considered here. $\ddot{R}$ and $\mathcal{A}_{cr}$ differ actually by three or even more orders of magnitude. This fact is confirmed by experimental observations. We stress that a slower bubble contraction, with respect to the spherical case, and the absence of the bouncing oscillations contribute to make shock formation impossible. The transformation of an AW into a shock is commonly seen as an instability property of the physical system. Therefore, we can say that a cylindrical geometry support the stability of the gas inside the bubble, regardless of the equation model employed to describe the phenomenon. This is in contrast with spherical bubbles [36]. However, differences in the critical amplitude can be observed in Figure 4 where the predictions of both RET theories are presented together. It turns

(a) **(b)**

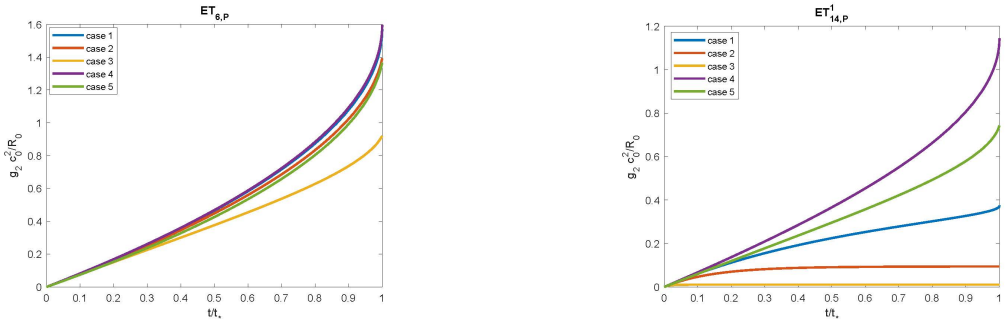

Fig. 3. A comparison between the RET 6-moment (a) and the 14-moment (b) theories: g_2 as a function of t/t_* for different physical parameters in the case of H_2O gas.

out that the critical values corresponding to $\mathrm{ET}^1_{14,P}$ differ by some magnitude orders from those calculated with $\mathrm{ET}_{6,P}$ system. This observation highlights the role played by the dissipation terms that were partially neglected in (21). The relevance of the dissipation is confirmed by Figure 4(b), where $\mathcal{A}_{cr}$ is plotted for different gas pressure (thus gas rarefaction) inside the bubble. Differences between an adiabatic ($\beta = 14/5$) and an isothermal ($\beta = 2$) bubble contraction are shown in Figure 5(a) for H_2O gas, while the role played by the bulk viscosity in the AW evolution is investigated in Figure 5(b) for a RET model with 6 moments, and $\beta = 14/5$. We remark that no significant differences can be observed in the $\mathcal{A}_{cr}$ values if $\mathrm{ET}^1_{14,P}$ is taken into account. On the other hand, a very large value of the ratio μ_b/ν should indirectly influence such a critical value, interfering with the bubble shrinkage. The numerical integrations were performed by Matlab and it was always verified that the unperturbed solutions are compatible with the hyperbolicity region of $\mathrm{ET}^1_{14,P}$ [53].

VII. CONCLUSIONS

The present work analyses the case of a contracting cylindrical bubble as an extension of some previous results in spherical symmetry [36]. Cylindrical bubbles were studied in the literature

(a) **(b)**

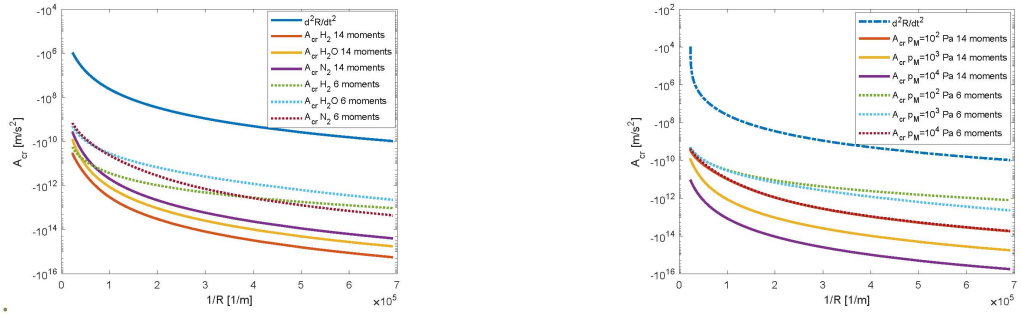

Fig. 4. A comparison between the $\mathcal{A}_{cr}$ predicted by RET 6-moment and the 14 moment theories: for different gases (a) and for different gas pressure p_M prescribed when $R = R_M$ for a H_2O gas (b). Here $\beta = 14/5$.

by many researchers due to their possible applications in several fields, such as medicine and engineering. For instance, it is known that a small spherical bubble expanding in a microchannel or in a micro-tube shifts to a cylindrical shape and starts to contract under the action of the liquid pressure or an oscillating acoustic signal.

To model AW propagation in this kind of bubbles, we refer here to RET theories, capable of describing phenomena far from equilibrium and of taking into account dissipation effects. Moreover, such PDE systems are of hyperbolic type, as required by a correct prediction of shock wave formation in AW theory [32, 36]. The comparison between $\mathrm{ET}_{6,P}$ and $\mathrm{ET}^1_{14,P}$ improves the comprehension of the role played by dissipation in AW evolution. In fact, in cylindrical symmetry the transformation of an AW into a shock is inhibited by the bubble dynamics, that turns out to be much slower than the spherical one. To our knowledge no experiments have ever revealed shock waves and what we present here is in complete agreement with these results. However, the presence of dissipation terms connected to heat flux and stress tensor could play a supplemental stabilizing effect, even under adiabatic assumptions. On the other hand, if the relaxation time

(a) **(b)**

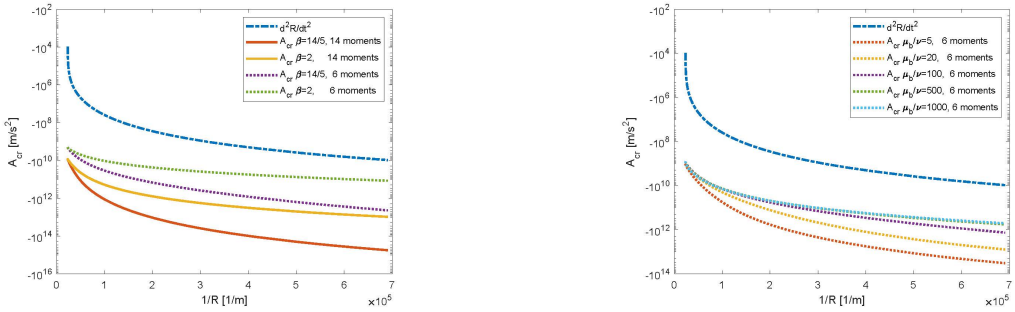

Fig. 5. A comparison between the $\mathcal{A}_{cr}$ predicted by RET 6-moment and the 14-moment theories for adiabatic ($\beta = 14/5$) and isothermal ($\beta = 2$) bubble contractions (a). In (b) the role of the bulk viscosity for a CO_2 gas modelled by RET 6-moment equations under adiabatic assumptions.

associated with the dynamic pressure (the unique relaxation time in $\mathrm{ET}_{6,P}$) is very large (as it could be in CO_2), the RET model with 6 moments is able to predict very high values of Π, but not to account for dissipative phenomena. Thus, it could be preferable to refer to the 14-moment system in this framework. The influence exerted by different gas properties, initial pressure and adiabatic/isothermal conditions are also investigated in the previous Sections.

In particular, it was possible to prove that in cylindrical geometry and in the presence of a non-zero bubble wall speed $\dot{R}$, both the dynamic pressure and the stress tensor do not vanish. This in accordance with the Navier-Stokes approximation, but in contrast with Euler gas model. As in [36], we stress that the dynamic pressure could reach very high values if the bulk viscosity and $\dot{R}$ are particularly high. In these circumstances, the total gas pressure ought to be taken into account in bubble radius evolution. Finally, we recall that in cylindrical geometry the stress tensor is not entirely negligible either, in contrast with spherical systems.

ACKNOWLEDGMENTS

This work was carried out in the framework of the activities of Gruppo Nazionale di Fisica Matematica GNFM-INdAM and was supported in part (F.B.) by the Italian research Project PRIN 2017 No. 2017YBKNCE "Multiscale phenomena in Continuum Mechanics: singular limits, off-equilibrium and transitions."

REFERENCES

[1] D. Lohse, "Bubble puzzles: From fundamentals to applications," *Phys. Rev .Fluids*, **3**, *110504* (2018).

[2] O. Lord Rayleigh, "On the pressure developed in a liquid during the collapse of a spherical cavity," *Phyl. Mag. Ser. 6*, **34**, 94 (1917).

[3] A. Prosperetti, "Bubble dynamics: a review and some recent results," *Applied Scientific Research*, **38**, 145 (1982).

[4] A. Prosperetti and Y. Hao, "Modelling of spherical gas bubble oscillations and sonoluminescence," *Phil. Trans. Royal Soc. A*, **357**, 203 (1999).

[5] B. Barber, R. Hiller, R. Löfstedt, S. Putterman, and K. Weninger, "Defining the unknowns of sonoluminescence," *Physics Reports*, **281**, 65 (1997).

[6] M. Brenner, S. Hilgenfeldt, and D. Lohse, "Single-bubble sonoluminescence," *Rev. Mod. Phys.*, **74**, 425 (2002).

[7] K. Suslick and D. Flannigan, "Inside a Collapsing Bubble: Sonoluminescence and the Conditions during Cavitation," *Annu. Rev. Phys. Chem.*, **59**, 659 (2008).

[8] W. Lauterborn and T. Kurz, "Physics of bubble oscillations," *Rep. Prog. Phys.*, **73**, *106501* (2010).

[9] H. Oguz and A. Prosperetti, "Dynamics of bubble growth and detachment from a needle," *J. Fluid Mech.*, **257**, 111 (1993).

[10] C. Delale, G. Tryggvason, and S. Nas, "Cylindrical bubble dynamics: Exact and direct numerical simulation results," *Phys.Fluids*, **20**, *040903* (2008).

[11] Y. Ilinskii, E. Zabolotskaya, T. Hay, and M. Hamilton, "Cylindrical bubble dynamics: Exact and direct numerical simulation results," *J. Acoust. Soc. Am.*, **132**, 1346 (2012).

[12] G. Bokman and O. Supponen, "Cavitation bubble dynamics in a shear-thickening fluid," *Phys. Rev. Fluids*, **7**, *023302* (2022).

[13] J. Duplat, "Dynamics of expansion and collapse of explosive two-dimensional bubbles," *J. Fluid Mech.*, **859**, 677 (2018).

[14] V. Papadopoulou, M. Tang, C. Balestra, R. J. Eckersley, and T. D. Karapantsios, "Circulatory bubble dynamics: From physical to biological aspects," *Adv. Colloid Interface Sci.*, **206**, 239 (2014).

[15] S. Cai, "Cavitation occurring in capillary tubes," *Phys. Lett. A*, **383**, 509 (2019).

[16] E. Zwann, S. Le Gac, K. Tsuji, and C. Ohl, "Cavitation occurring in capillary tubes," *Phys. Rev. Lett.*, **98**, *254501* (2007).

[17] P. Quinto-Su, K. Y. Lim, and C. D. Ohl, "Cavitation bubble dynamics in microfluidic gaps of variable height," *Phys. Rev. E*, **80**, *047301* (2009).

[18] P. Quinto-Su and C. D. Ohl, "Interaction between two laser-inducedcavitation bubbles in a quasi-two-dimensional geometry," *J. Fluid Mech.*, **633**, 425 (2009).

[19] S. Gonzalez-Avila, E. Klaseboer, B. Khoo, and C. Ohl, "Cavitation bubble dynamics in a liquid gap of variable height," *J. Fluid Mech.*, **682**, 241 (2011).

[20] G. Sinibaldi, A. Occhicone, F. A. Pereira, D. Caprini, L. Marino, F. Michelotti, and C. Casciola, "Laser induced cavitation: Plasma generation and breakdown shockwave," *Phys. Fluids*, **31**, *103302* (2019).

[21] G. Boillat, *La propagation des ondes*, Gauthier-Villars, Paris, France (1965).

[22] G. Boillat and T. Ruggeri, "On the evolution of weak discontinuities for hyperbolic quasi-linear systems," *Wave Motion*, **1**, 149 (1979).

[23] T. Ruggeri, "Stability and discontinuity waves for symmetric hyperbolic systems," *Nonlinear wave motion ed. A. Jeffrey, Longman,*, 148–161 (1989).

[24] K. Lindsay and B. Straughan, "Acceleration waves and second sound in a perfect fluid," *Arch. Ration. Mech. Anal.*, **68**, 54 (1978).

[25] P. M. Jordan and B. Straughan, "Acoustic acceleration waves in homentropic Green and Naghdib gases," *Proc. R. Soc. A*, **462**, 3601 (2006).

[26] T. Ruggeri and L. Seccia, "Hyperbolicity and wave propagation in extended thermodynamics," *Meccanica*, **24**, 127 (1989).

[27] R. Bowen and M. L. Doria, "Effect of diffusion on the growth and decay of acceleration waves in gases," *J. Acoust. Soc. America*, **53**, 75 (1973).

[28] A. Muracchini and L. Seccia, "Thermo-acceleration waves and shock formation in extended thermodynamics of gravitational gases," *Contin. Mech. Thermodyn.*, **1**, 227 (1989).

[29] A. Muracchini and T. Ruggeri, "Acceleration waves, shock formation and stability in a gravitating atmosphere," *Astrophys. Space Sci.*, **153**, 127 (1989).

[30] E. Barbera and G. Valenti, "Kawashima condition and acceleration waves for binary non reacting mixtures," *Acta Mech.*, **187**, 203 (2006).

[31] F. Brini and L. Seccia, "Acceleration waves in rational extended thermodynamics of rarefied monatomic gases," *Fluids*, **5**, *139* (2020).

[32] I. Müller, "Extended Thermodynamics: a theory of symmetric hyperbolic field equations," *Entropy*, **10**, 477 (2008).

[33] T. Ruggeri and M. Sugiyama, *Classical and Relativistic Rational Extended Thermodynamics of gases*, Springer, New York (2021).

[34] I. Müller and T. Ruggeri, *Rational Extended Thermodynamics*, Springer, New York (1998).

[35] T. Arima, T. S., T. Ruggeri, and M. Sugiyama, "Extended thermodynamics of dense gases," *Contin. Mech. Thermodyn.*, **24**, 219 (2012).

[36] F. Brini and L. Seccia, "Acceleration waves and oscillating gas bubbles modelled by rational extended thermodynamics," *Proc. R. Soc. A*, **478**, *20220246* (2022).

[37] S. Putterman and W. K.R., "Sonoluminescence: How bubbles turns sound into light," *Annu. Rev. Fluid Mech.*, **32**, 445 (2000).

[38] H. Lin, B. Storey, and A. Szeri, "Inertially driven inhomogeneities in violently collapsing bubbles: the validity of the Rayleigh-Plesset equation," *J. Fluid Mech.*, **452**, 145 (2020).

[39] A. Prosperetti, "The thermal behaviour of oscillating gas bubbles," *J. Fluid Mech.*, **222**, 587 (1991).

[40] G. Zhou and A. Prosperetti, "Modelling the thermal behaviour of gas bubbles," *J. Fluid Mech.*, **901**, *R3* (2020).

[41] C. Wu and P. Roberts, "Shock-wave propagation in a sonoluminescencing gas bubble," *Phys. Rev. Lett.*, **70**, 3424 (1993).

[42] V. Vuong and A. Szeri, "Sonoluminescence and diffusive transport," *Phys. Fluids*, **8**, 2354 (1996).

[43] H. P. Greenspan and A. Nadim, "On sonoluminescence of an oscillating gas bubble," *Phys. Fluids A*, **5**, 1065 (1993).

[44] C. Borgnakke and P. Larsen, "Statistical collision model for Monte Carlo simulation of polyatomic gas mixture," *J. Comput. Phys.*, **18**, 405 (1975).

[45] J. Bourgat, L. Desvillettes, T. P. L., and P. B., "Microreversible collisions for polyatomic gases," *Eur. J. Mech. B/Fluids*, **13**, 237 (1994).

[46] C. Truesdell, "The physical components of vector and tensor," *ZAMM*, **33**, 345 (1953).

[47] T. Arima, E. Barbera, F. Brini, and M. Sugiyama, "The role of the dynamic pressure in stationary heat conduction of a rarefied polyatomic gas," *Phys. Lett. A*, **378**, 2695 (2014).

[48] W. Haynes, *CRC Handbook of Chemistry and Physics*, 92nd Edition CRC Press (2011).

[49] M. Cramer, "The physical components of vector and tensor," *Phys. Fluids*, **24**, *066102* (2012).

[50] S. Kosuge and K. Aoki, "Shock-wave structure for a polyatomic gas with large bulk viscosity," *Phys. Rev. Fluids*, **3**, *023401* (2018).

[51] B. Sharma and R. Kumar, "Estimation of bulk viscosity of dilute gases using a nonequilibrium molecular dynamics approach," *Phys. Rev. E*, **100**, *013309* (2019).

[52] E. Kustova, M. Mekhonoshina, and A. Kosareva, "Relaxation processes in carbon dioxide," *Phys. Fluids*, **31**, *046104* (2019).

[53] F. Brini and T. Ruggeri, "Hyperbolicity of first and second order extended thermodynamics theory of polyatomic rarefied gases," *Int. J. Non-lin. Mech.*, **124**, *103517* (2020).